JOURNAL OF MATERIALS SCIENCE: MATERIALS IN MEDICINE 7 (1996) 447–455

Transmission electron microscopy study of a dental gallium alloy

A. E. GUNNÆS, A. OLSEN, H. HERØ*
Centre for Materials Research/Department of Physics, University of Oslo, Gaustadalleen 21, 0371 Oslo, Norway
**NIOM, Scandinavian Institute of Dental Materials, P.B. 70, 1344 Haslum, Norway*

Analytical transmission electron microscopy (TEM) studies of a dental gallium alloy have been carried out. This commercial Ga alloy was made by triturating a Ag–Sn–Cu-rich alloy powder with a liquid Ga alloy containing Ga, In and Sn. Ga alloys are of increasing interest as an alternative to amalgam. The dental material studied in the present work was found to be a composite consisting of remaining, undissolved particles from the Ag-based alloy powder in a matrix of reaction products with the liquid Ga alloy. The phases in the matrix and the remaining Ag-based alloy particles have been identified by electron diffraction, high resolution electron microscopy and energy dispersive X-ray spectroscopy. The following phases were identified: orthorhombic Ag_3Sn, cubic γ-Cu_9Ga_4, cubic Ag_9In_4, tetragonal β-Sn and hexagonal Ag_2Ga. In addition to these well-known phases Ga-rich regions of Cu–Ga were observed consisting of an intergrowth of the tetragonal $CuGa_2$ and one of the cubic γ-Cu_9Ga_4 phases.

1. Introduction

Gallium alloys as a filling material and a replacement for amalgam was suggested for the first time by Puttkammer in 1928 [1]. Smith and Caul in 1956 [2] were the first to produce Ga alloys for dental purposes. In recent years the interest in Ga alloys for this application has increased because of the risk of environmental pollution from amalgam and the controversy about possible toxic effects of Hg in amalgam fillings [3].

In Japan a commercial Ga alloy (Gallium Alloy GF, Tokuriki Honton, Japan) has been on the market for some time. This alloy has also been approved by the health authorities of Japan. The composition of the Ag-based spherical alloy powder of this product is similar to that of an ordinary high Cu alloy for amalgam, except that it contains as much as 9 wt % Pd. A liquid Ga alloy is to be mixed with this alloy powder in the same way as for amalgam.

Ga has a melting point as low as 29.8 °C [4]. When it is alloyed with 19 wt % In and 16 wt % Sn the melting point is reduced to below 10 °C. An initially plastic material is formed by mixing this liquid with the alloy powder. Like amalgam it can be condensed into a prepared cavity where it then sets to a solid. The handling characteristics are reported to be inferior to that of amalgam [5], but can be overcome by special techniques and equipment.

Ga Alloy GF and other Ga alloys have been found to have similar mechanical properties to that of leading high copper amalgams [6]. The corrosion properties of Ga alloys as tested in vitro, however, have been questioned [7]. Furthermore, Okabe *et al.* [8] and Jørgensen *et al.* [9], have reported values for setting expansion of the Ga Alloy GF that are clearly above the maximum level accepted in ISO 1559 "Dental alloys for amalgams" [10]. This effect has not been reported for other Ga alloys. The reason for this anomalous behaviour of Gallium Alloy GF is unknown.

These properties of Ga alloys must be reflected in their structures. Hence, optimization of their properties will benefit from an adequate knowledge of the structures of the alloys. Okabe *et al.* [6] and Herø et al. [11] found, by X-ray diffraction and scanning electron microscopy (SEM) studies, Ga alloy GF to consist of unconsumed spherical particles of the alloy powder embedded in a matrix consisting of Ag_9In_4, Ag_2Ga and β-Sn grains. A reaction layer of $CuGa_2$ and Cu_9Ga_4 was surrounding the pre-alloy particles. A similar structure of Ga alloys made on the basis of spherical alloys with high Cu content intended for amalgam has been observed by Okabe *et al.* [8].

A Ag-based alloy powder intended for amalgam has been reported, on the basis of X-ray diffraction, to consist of an orthorhombic Ag_3Sn phase [12]. Similarly, Herø *et al.* [11] have, for the alloy powder made for gallium alloy GF, also observed indications of a hexagonal Ag_3Sn phase by using X-ray diffraction.

The aim of the present work was to characterize the microstructure of the gallium alloy GF further by transmission electron microscopy. The main purpose of this TEM study was to identify the phases present in the alloy by using selected area electron diffraction, high resolution electron microscopy and energy dispersive X-ray spectroscopy. This Ga alloy contains as

0957–4530

many as seven different elements, and many phases and a complex microstructure were expected to be found. Because the same dental Ga alloy has previously been studied by Herø *et al.* [11] using X-ray powder diffraction, a comparison of the results found in the present TEM investigation and the X-ray study will be made.

2. Experimental procedures

2.1. Materials

The dental Ga alloy GF was made by triturating a Ag-based alloy powder with a liquid Ga alloy. The powder to liquid ratio was 1:0.65 by weight. The compositions of the applied alloy powder and the liquid Ga alloy for the commercial Ga alloy GF according to the manufacturer are given in Table I. The dental material is the same as designated Ag-based GF powder in the paper by Herø *et al.* [11] and more details about the material preparation can be found in their paper.

2.2. Sample preparation for TEM

Mechanically polished samples with thickness of the order of 50 μm and diameters less than 3 mm were the starting materials for the TEM study. The samples were first mechanically thinned by dimpling with a Gatan dimple grinder model 656. During the dimpling procedure 15 and 1 μm diamond paste and polishing wheels were used. The dimpling was stopped when a tiny hole was seen in the specimen. Because the specimens were less than 3 mm in diameter (which is the size of the TEM specimen holder) they were glued to Cu grids. The central part of the Cu grids was removed before the samples were glued, so the Cu grids would not interfere during the TEM study. After the dimpling procedure the specimens were thinned with Ar ions at 4 kV for about 2 h in a Gatan Dual ion-mill 600. The gun currents were 0.5 mA per gun and the specimen surface was oriented 12° relative to the incident ion beams.

2.3. Analytical electron microscopy

The dental Ga alloy was examined at 200 kV in a JEOL 2000 FX transmission electron microscope equipped with a Tracor Northern X-ray detector and a SCANDNORDAX X-ray analyser. In order to characterize the microstructure of the dental Ga alloy, a combination of bright field (BF), dark field (DF), high resolution electron microscopy (HREM), selected area electron diffraction (SAD) and energy dispersive X-ray spectroscopy (EDS) was used. From the X-ray intensity data of the EDS analyses, the concentration ratios between the elements in each crystalline phase ere found by using the Cliff-Lorimer equation [13]:

$$\frac{C_1}{C_2} = \frac{K_{1Si} * I_1}{K_{2Si} * I_2} \quad (1)$$

C_1 and C_2 are the concentrations of the elements 1 and 2, respectively, given in at %. K_{1Si} and K_{2Si} are the K-factors of the elements relative to Si. I_1 and I_2 are the intensities of the X-ray peaks from element 1 and 2 in the EDS spectrum. The K_{iSi}-factors may vary from instrument to instrument depending on the type of detector and specimen surroundings. The K_{iSi}-factors are also depending on the accelerating voltage, but are independent of the specimen thickness and the composition as long as the thin film approximation is valid. The K_{iSi}-factors used in the present investigation were taken from Olsen [14], where experimental and calculated K_{iSi}-factors for 200 kV are given as a function of the atomic number Z of element i. In Table II the K_{iSi}-factors are given with their standard deviations is parentheses.

TABLE I Material compositions according to the Ga alloy GF manufacturer

Ag-based alloy powder					
Element	Ag	Sn	Cu	Pd	Zn
Weight %	50	25.7	15	9	0.3
Liquid GA alloy					
Element		Ga	In	Sn	
Weight %		65	19	16	

TABLE II K_{iSi}-factors (with their accuracies in parenthesis) at 200 kV used in the Cliff–Lorimer equation. (Equation 1)

Element	K_{iSi}
Cu	0.59 (0.02)
Zn	0.60 (0.02)
Ga	0.61 (0.02)
Pd	1.35 (0.03)
Ag	1.50 (0.03)
In	1.77 (0.03)
Sn	2.06 (0.03)

3. Results and discussion

The dental Ga alloy GF was found to be a composite consisting of undissolved particles from the Ag-based alloy powder surrounded by a matrix of reaction products. The phases in the matrix and the remaining parts of the Ag-based alloy particles have been identified and are described in the following.

3.1. The Ag_3Sn phase

The remaining, undissolved Ag-based alloy powder particles were found to consist of Ag_3Sn grains (Fig. 1a). No Cu-Sn containing particles were observed. In Fig. 1b a typical EDS spectrum from the Ag_3Sn phase is presented. The Ag $L_{\beta 2}$ (3.347 keV) and Sn L_α (3.443 keV) peaks was difficult to distinguish because the energy difference is at the limit of the energy resolution (145 eV at 5.894 keV) of the applied energy dispersive spectrometer. This made it difficult to determine the composition ratio between the two elements Ag and Sn by use of the Cliff–Lorimer equation (Equation 1).

As shown in Fig. 1a the diameter of the grains are in the order of 0.2–0.75 μm. Larger Ag_3Sn grains were,

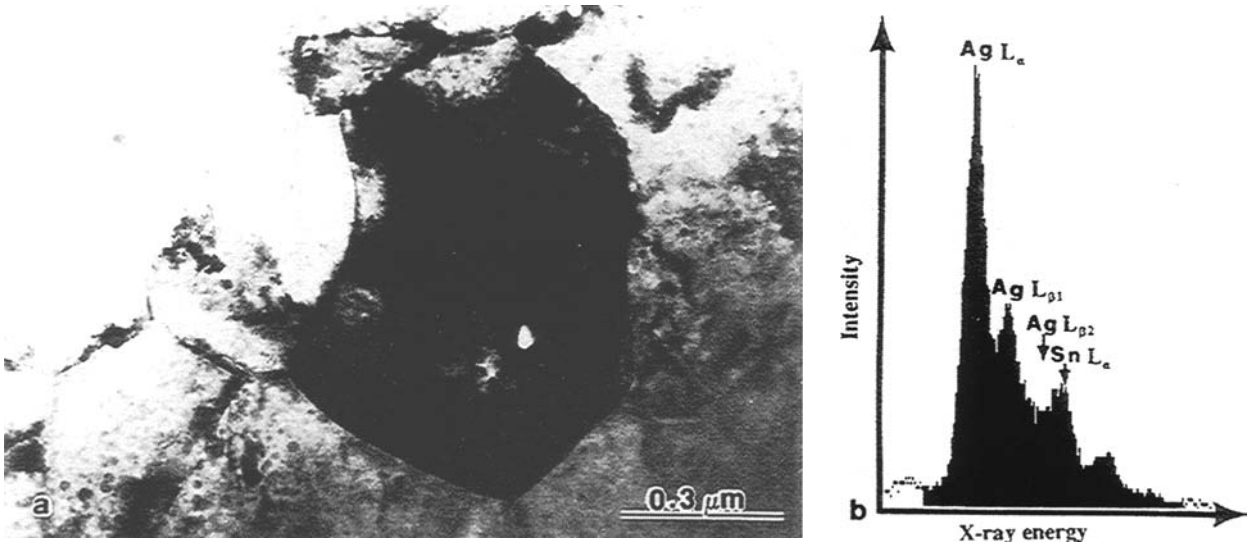

Figure 1 (a) BF image showing Ag_3Sn grains, and (b) corresponding EDS spectrum showing the nearly overlapping Ag $L_{\beta1}$ and Sn L_α peaks.

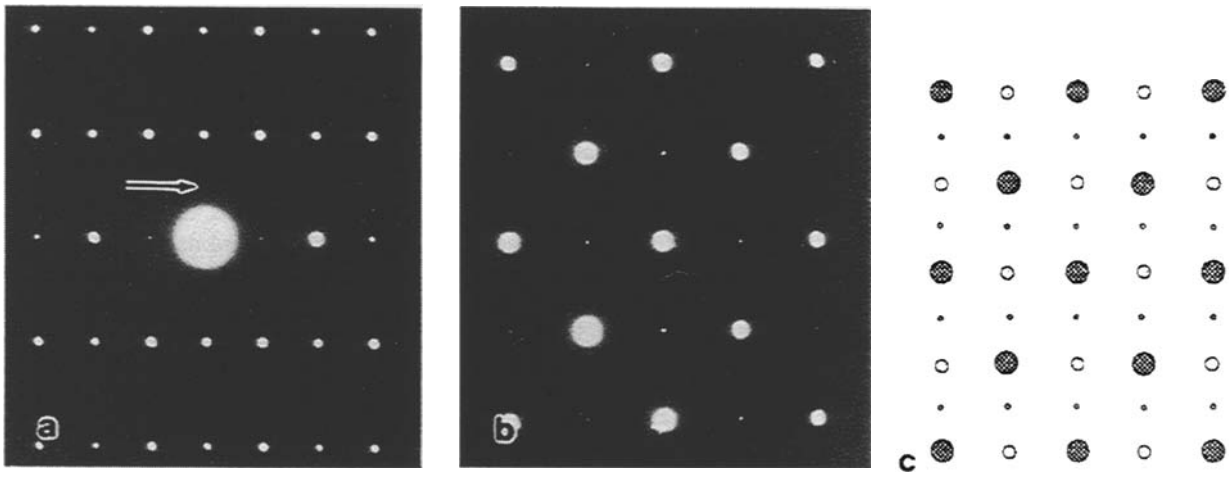

Figure 2 SAD patterns of the Ag_3Sn phase. (a) Experimental [1 0 0] projection with weak reflections indicated by arrow; (b) experimental [0 1 1] projection; and (c) corresponding schematic drawing.

however, also seen in the particles. In Fig. 1a some "dots" can be seen in the image. The "dots" have been examined by use of EDS and SAD. According to the SAD analyses the "dots" do not contribute to any extra reflections in the diffraction patterns from Ag_3Sn. In conclusion the "dots" are not particles, but may rather be caused by the electron beam.

The SAD patterns (Fig. 2) taken of the Ag_3Sn phase correspond to an orthorhombic structure with space group Pmmn and are consistent with the cell dimensions $a = 0.5968$ nm, $b = 0.47802$ nm and $c = 0.51843$ nm as published by Fairhurst and Cohen based on single-crystal X-ray diffraction [12]. In Fig. 2a the high symmetry projection [1 0 0] is shown. Two types of reflections can be recognized. On the positive film one type of reflections can easily be seen. The other type is weak and more difficult to see (indicated by arrow). In the [0 1 1] SAD pattern (Fig. 2b) three type of reflections can be recognized. The strongest reflections can easily be seen. In addition there are weak and even weaker reflections in this projection as indicated in the schematic drawing in Fig. 2c. These very weak reflections are difficult to see on the positive film and may be even more difficult to recognize by X-ray powder diffraction.

The cell dimensions found in the present investigation differ from the corresponding values of the orthorhombic Ag_3Sn phase as given by Herø *et al.* [11]. They found that the dental material consists of a Ag-Sn rich phase which most likely is hexagonal or possibly orthorhombic. By use of X-ray powder diffraction the cell dimensions of the orthorhombic Ag_3Sn phase were found to be consistent with $a = 0.4801$ nm, $b = 0.4780$ nm and $c = 0.3048$ nm. This c-axis is approximately half the a-axis value as found in the present investigation. The discrepancy may be due to the very weak reflections in the electron diffraction patterns giving the doubling of the 0.3048 nm axis. The hexagonal ζ-Ag_3Sn phase also reported by Herø *et al.* [11] based on X-ray powder diffraction for the same dental material was not observed in the present TEM study.

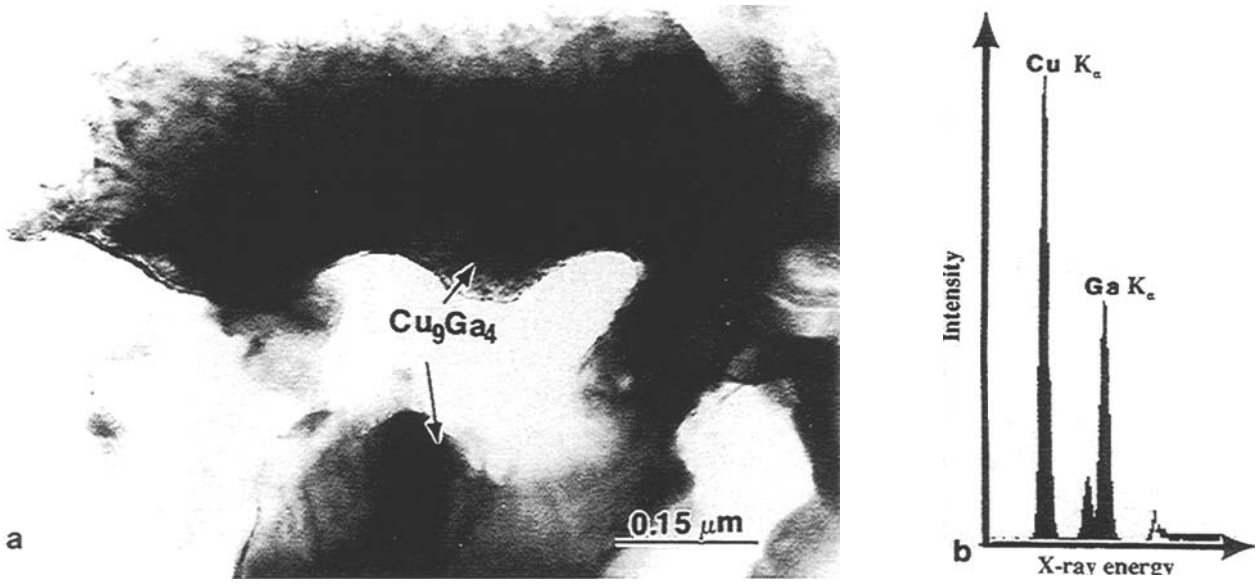

Figure 3 (a) BF image showing region of the Cu_9Ga_4 phase with (b) the corresponding EDS spectrum.

3.2. Cu-Ga phases

In the zones between the remaining powder particles and the matrix two types of Cu-Ga regions were found by analytical TEM: Cu-rich and Ga-rich.

The Cu-rich phase was identified to be consistent with one of the cubic γ-Cu_9Ga_4 phases with space group $P\bar{4}3m$ and cell dimension $a = 0.8747$ nm as given by Stokhuyzen *et al.* [15]. The Cu_9Ga_4 phase does not seem to have a characteristic grain structure (Fig. 3a). The typical size of the regions is of the order of 1.5 μm, but some grains may be larger than 1.5 μm. The EDS spectrum in Fig. 3b was recorded from the area shown in Fig. 3a. By using the Cliff–Lorimer equation (Equation 1) the composition ratio between Cu and Ga was found to be approximately 2. According to Massalski *et al.* [16] the γ_1-Cu_9Ga_4 phase has a composition range of 30–35 at % Ga. Thus, the experimental composition value of the present dental material is in good agreement with this. According to Herø *et al.* [11] the X-ray diffraction indicates a minor fraction of the cubic Cu_9Ga_4. In Fig. 4a, b and c three different SAD patterns are shown: the [0 0 1], [1 1 $\bar{1}$] and [1 1 $\bar{2}$] projections, respectively.

The Ga-rich regions have a composition about 60 at % Ga as found by EDS analyses. Fig. 5 shows three different SAD patterns taken of this Ga-rich regions. These diffraction patterns have some similarities with the SAD patterns from the Cu_9Ga_4 phase shown in Fig. 4. There are, however, some very important differences both in the position and the intensity of the reflections. In the SAD patterns shown in Fig. 5 there are large differences in intensity between the strong and weak reflections whereas the SAD patterns shown in Fig. 4 there is much less difference in intensity between the strong and weak reflections.

Fig. 6 shows three other SAD patterns from the Ga-rich Cu-Ga regions. In these patterns the shortest distance between the reflections corresponds to a *d*-value of 1.75 nm. It is also to be noticed that the distance between the strong reflections in all the SAD patterns from this phase is divided into three by weak reflections. This could indicate that the structure of the Ga-rich Cu-Ga regions has a unit cell with dimensions three times a basic cell.

BF, DF and HREM show, however, that these Ga-rich regions are intergrowths of two phases. In Fig. 7a the BF image shows grains of the Ga-rich Cu-Ga regions. The grains have diameters of the order of 1 μm. The contrast is a modulated type with the modulation vector normal to the *c*-axis. One should notice that the contrast is different in different grains and depends on the crystal orientation. The contrast is also different from the image contrast of the Cu_9Ga_4 phase shown in Fig. 3a.

In the Ga-rich part of the phase diagram relatively few phases have been reported in the literature. The φ-phase reported by Weibke [17] has a composition near 56 at % Ga and exists below 249 °C. This phase was subsequently reported by Zintl and Treusch [18] to be tetragonal with cell dimensions $a = 0.2836$ nm, $c = 0.5847$ nm and space group P4mm. They observed that this phase was homogeneous at 58 at % Ga, but according to them the unit cell contains three atoms. Therefore they suggested that the composition of this phase should be $CuGa_2$ and the atomic positions Cu (1b) $\frac{1}{2}$ $\frac{1}{2}$ 0.27, Ga (1b) $\frac{1}{2}$ $\frac{1}{2}$ 0.70, Ga (1a) 0 0 0. Subsequently Betterton and Hume-Rothery [19] found that this phase does not contain 56 at % Ga as reported by Weibke [17], but corresponds almost exactly to the composition $CuGa_2$. They called this phase the θ-phase. The cell dimensions of this phase were later determined by El-Boragy and Schubert [20] to be $a = 0.2830$ nm, $c = 0.5839$ nm. However, they concluded that the structure has the $FeSi_2$-type and the space group P4/mmm. According to them the atomic positions are: Cu(1a) 0 0 0, Ga(2h) $\frac{1}{2}$ $\frac{1}{2}$ 0.295. In the phase diagram published by Massalski *et al.* [16], the φ-phase has been called the ε-phase.

An EDS spectrum of this Ga-rich region is shown in Fig. 7b. By using the Cliff–Lorimer equation

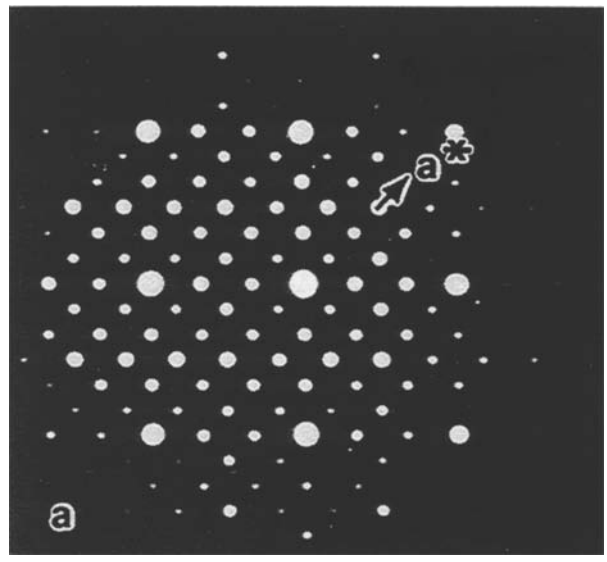

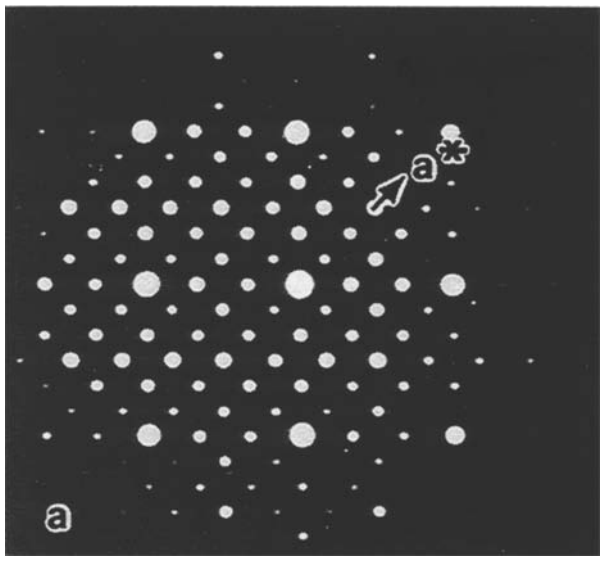

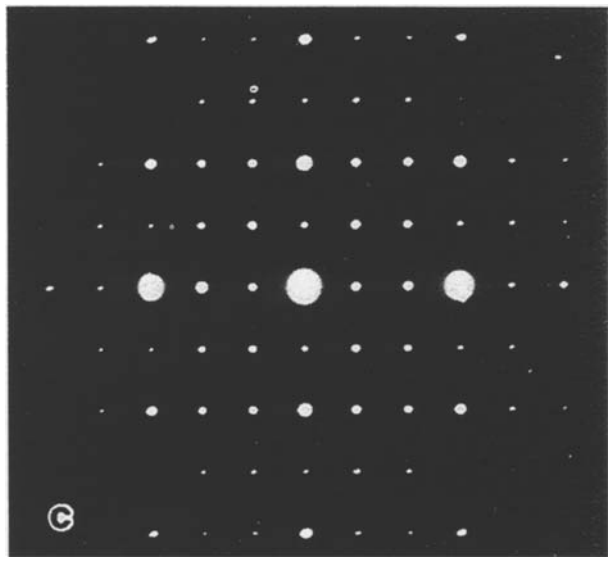

Figure 4 SAD patterns of the Cu_9Ga_4 phase. (a) [0 0 1]; (b) [1 1 1]; and (c) [1 1 0] projections.

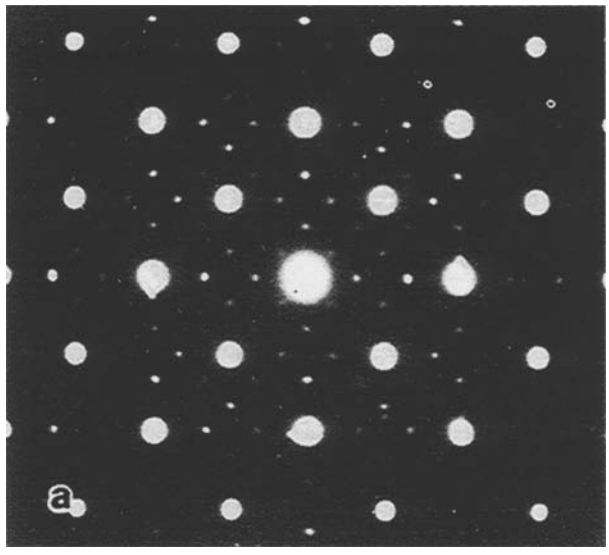

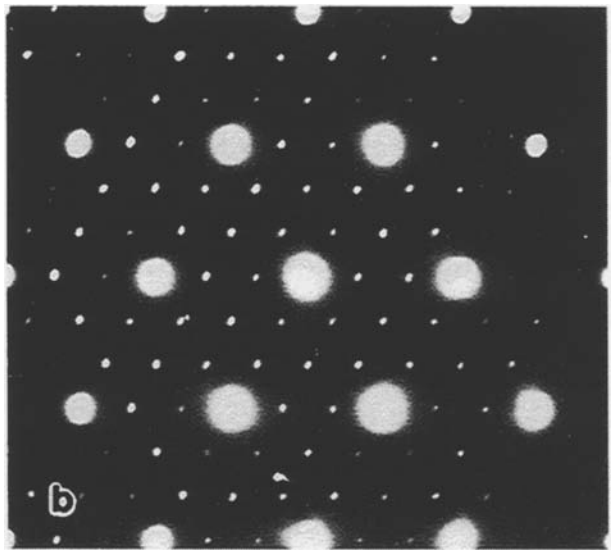

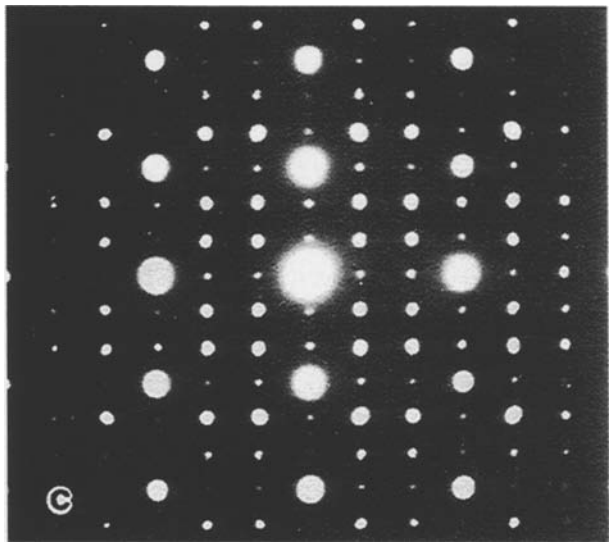

Figure 5 SAD patterns taken from the Ga-rich Cu-Ga phase showing similarities with the projections of the Cu_9Ga_4 seen in Fig. 4.

(Equation 1) the composition was found to be approximately 60 at % Ga. In the Cu-Ga phase diagram [16] this would be at the left-hand side of the ε phase. A comparison of the results in the present investigation with the literature shows that the pr esent Ga-rich regions are intergrowths of two Cu-Ga phases, the tetragonal $CuGa_2$ and one of the cubic γ-Cu_9Ga_4 phases. A more detailed analysis of these regions will be published elsewhere.

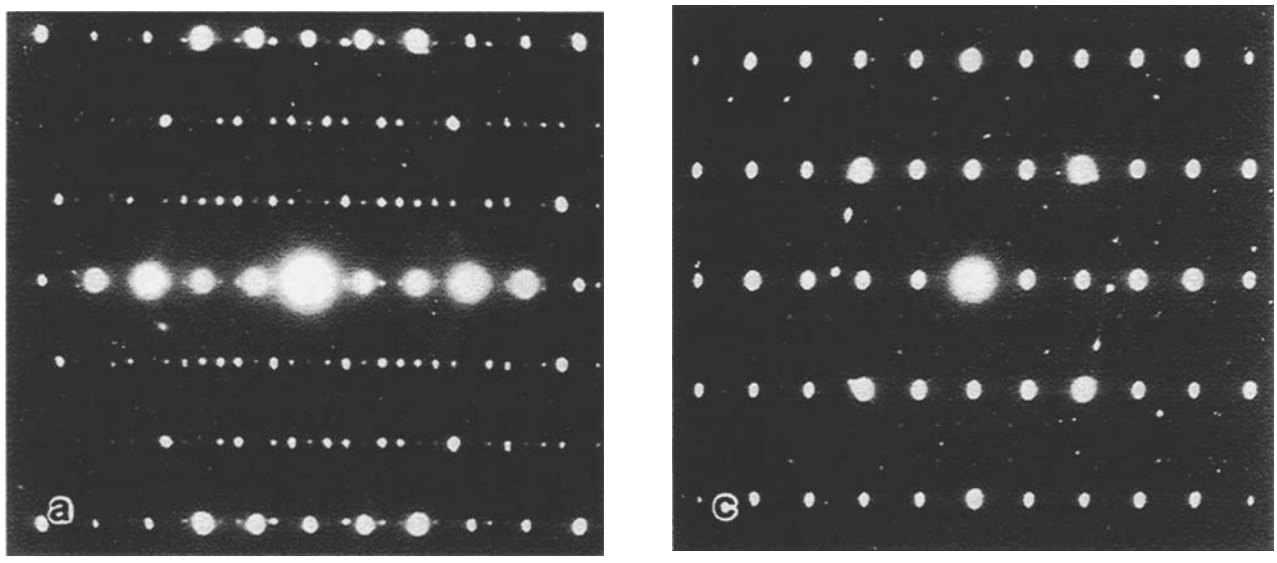

Figure 6 SAD patterns taken the Ga-rich Cu-Ga regions showing dense rows of reflections.

According to Herø *et al.* [11] the Ga content of the Ga-rich phase θ-Cu(Pd) Ga_2 is 77.7 at %. In addition they also reported 7.9 at % Pd in this phase. Pd was, however, not detected in the present work.

3.3. The Ag_9In_4 phase

The matrix in the dental Ga alloy was found to consist mainly of the Ag_9In_4 phase. The regions with the Ag_9In_4 phase are found to consist of large grains containing subgrains. The exact size of the grains was not determined. The SAD patterns correspond to a cubic structure with space group $P\bar{4}3m$ and cell dimensions consistent with $a = 0.9922$ nm as published

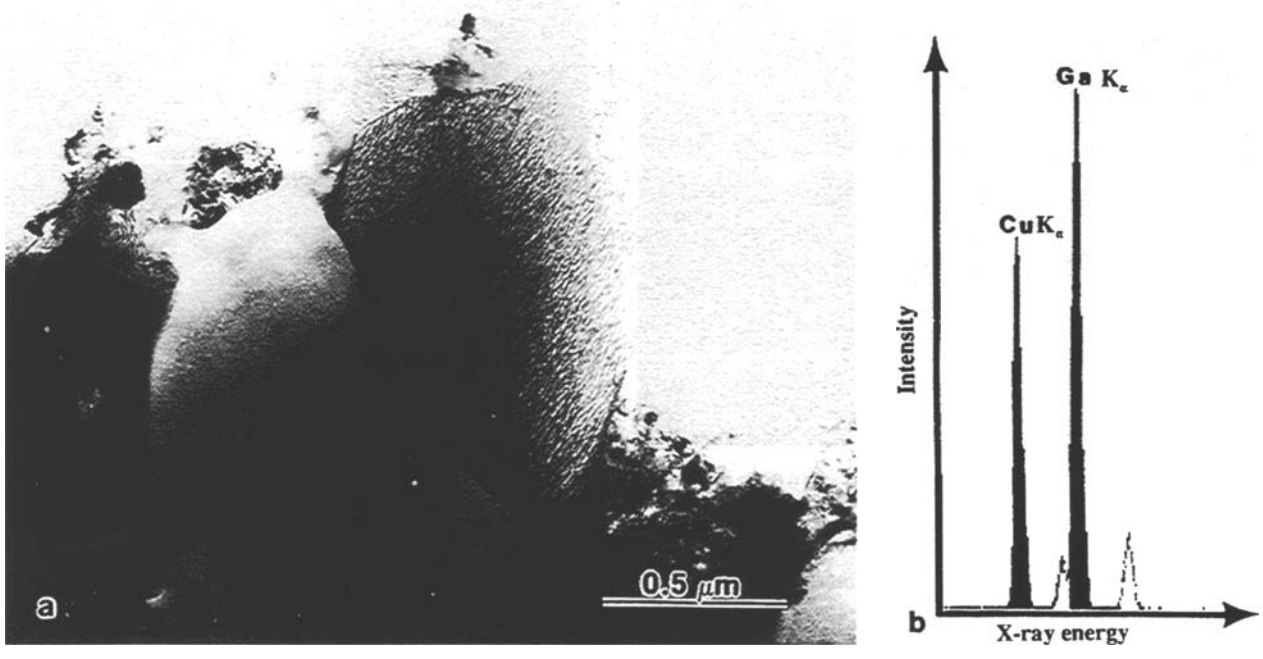

Figure 7 (a) BF image showing grains of the Ga-rich Cu-Ga phase and (b) corresponding EDS spectrum.

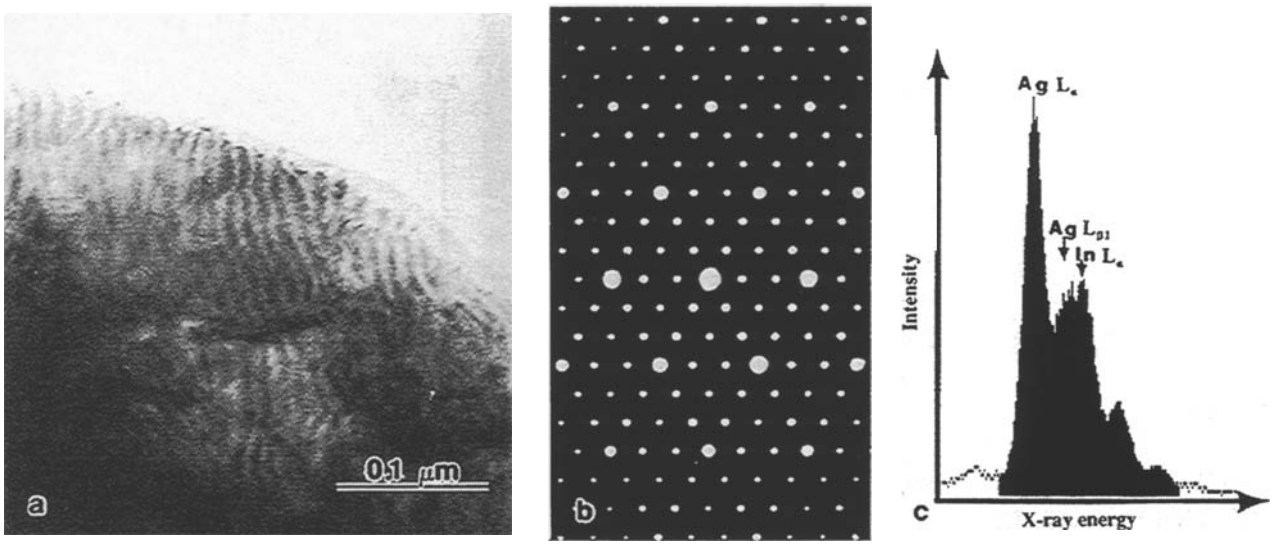

Figure 8 (a) HREM image of the Ag_9In_4 phase seen in the [1 1 1] orientation. (b) Corresponding SAD pattern; and (c) EDS spectrum showing the Ag $L_{\beta1}$ and In L_α peaks.

by Brandon *et al.* [21]. Fig. 8 shows a HREM image (a) and its corresponding SAD pattern (b). As may be seen from the HREM image the Ag_9In_4 phase seems to show similar modulated contrast features as the Ga-rich Cu-Ga regions. This feature is, however, not so characteristic as for the Ga-Cu case.

The EDS spectrum of the Ag_9In_4 phase (Fig. 8c) looks very similar to the EDS spectrum from the Ag_3Sn phase (Fig. 1b). As shown in Fig. 8c the Ag $L_{\beta1}$ (3.150 keV) and In L_α (3.286 keV) peaks overlap. Just as for the Ag_3Sn phase this makes it difficult to determine the ratio between the two elements by use of the Cliff–Lorimer equation (Equation 1). The modulated contrast may be due to an intergrowth of Ag_9In_4 and Ag_3Sn. These two phases have very similar dimensions in the [1 0 0] projections. The Ag_9In_4 is cubic with cell dimensions $a = 0.9922$ nm [21] and the periodicity along the $\langle 0\,1\,1\rangle$ directions is 1.4032 nm. The Ag_3Sn phase is orthorhombic with cell dimensions $a = 0.5968$ nm, $b = 0.47802$ nm and $c = 0.51843$ nm [12]. The periodicity along the $\langle 0\,1\,1\rangle$ directions is 0.7051 nm. The angle between [0 1 1] and [0 1 $\bar{1}$] is 94.64°, whereas the corresponding angle in the Ag_9In_4 phase is 90°. Therefore in the [1 0 0] projections there is a simple relationship between the lattices of the two phases: Ag_3Sn $\langle 0\,1\,1\rangle \approx Ag_9In_4$ $\frac{1}{2}\langle 0\,1\,1\rangle$. These two phases are also difficult to distinguish by EDS due to the following overlaps:

$$\text{Ag } L_{\beta2}(3.347\text{ keV}) \approx \text{In } L_{\beta1}(3.487\text{ keV}) \approx \text{Sn } L_\alpha(3.443\text{ keV})$$

$$\text{In } L_{\beta2}(3.713\text{ keV}) \approx \text{Sn } L_{\beta1}(3.662\text{ keV})$$

3.4. The Sn phase

Almost pure Sn was found to cover large areas. The Sn phase was found in contact with the Ag_9In_4 and sometimes the Ga-Cu phases. The Sn phase corresponds to the tetragonal β-structure published by Deshpande and Sirdeshmukh [22] with space group $I4_1/amd$ and cell dimensions $a = 0.58318$ nm and $c = 0.31819$ nm. In Fig. 9a DF image taken of the Sn phase is shown. Some small particles in the Sn phase can be seen. The EDS spectra taken from these

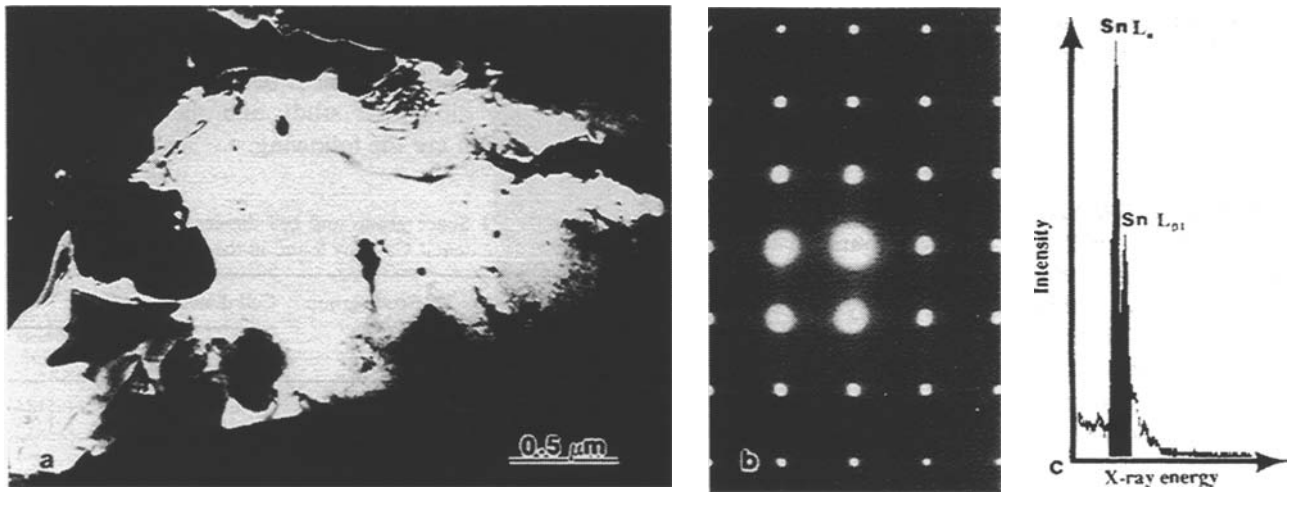

Figure 9 (a) DF image of the Sn phase taken with the 2 0 0 reflection. (b) Corresponding SAD pattern ([1 0 0] projection); and (c) EDS spectrum.

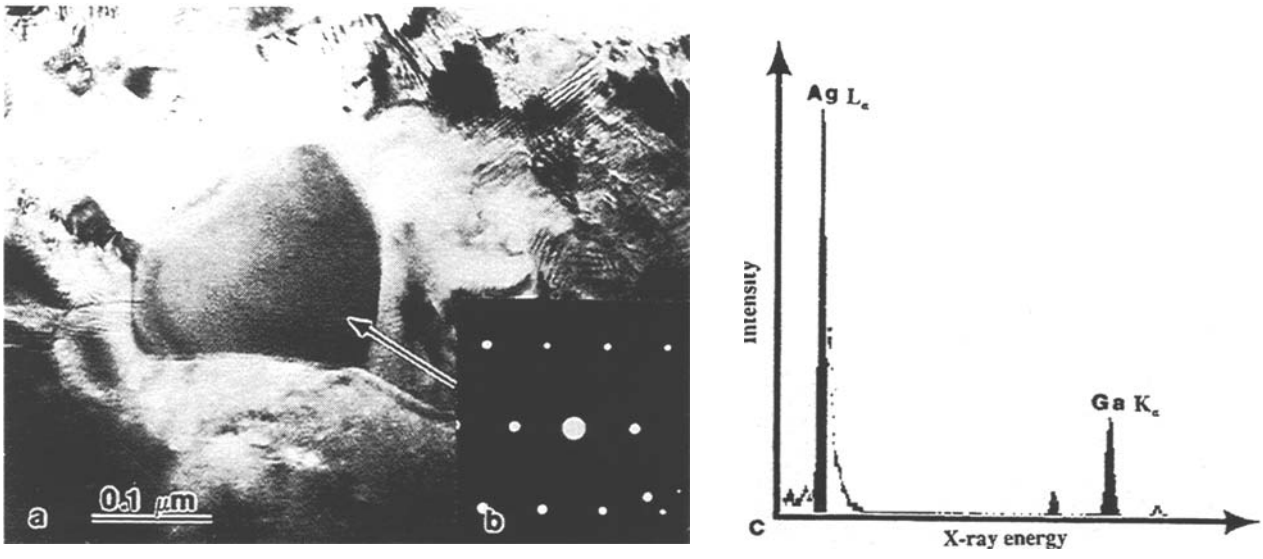

Figure 10 (a) BF image; (b) SAD pattern; and (c) EDS spectrum taken from the Ag_2Ga phase.

particles show that they are Ag-rich, but no further analyses were carried out in order to determine more accurately the Ag content. The [1 0 0] SAD patterns of the Sn regions show diffuse streaks along the ⟨1 0 0⟩ directions (Fig. 9b). These streaks are not due to precipitates, but may be due to thermal vibrations of the Sn atoms. Such thermal diffuse streaks in SAD patterns from Sn are well known [23] and are due to an intersection between diffuse walls of scattered electrons and the Ewald sphere. Both the EDS spectrum (Fig. 9c) and the SAD pattern (Fig. 9b) with diffuse streaks are very characteristic of the Sn phase found in the present dental material.

3.5. The Ag_2Ga phase

A Ag_2Ga phase was also observed in the matrix of the dental material. This phase was found to be consistent with a hexagonal structure with space group $P\bar{6}$ and cell dimensions $a = 0.77677$ nm and $c = 0.28778$ nm as published by Stratton and Kitchingman [24]. In Fig. 10 a BF image (a) of the Ag_2Ga phase with its corresponding SAD pattern (b) is shown. The area in Fig. 10a consists of several small grains. Large amount of moiré patterns caused by overlapping grains can be seen. The characteristic EDS spectrum (Fig. 10c) from the Ag_2Ga phase was recorded from the region shown in Fig. 10a.

3.6. The presence of Pd and Zn

No indications of Pd or Zn were found in the EDS analyses. Pd has previously been found associated with Cu and Ga in this dental Ga alloy by use of EDS in SEM [11]. Pd should be seen in the present investigation if the Pd concentration is as high as 7.9 at % as reported by Herø *et al.* [11] for the Ga rich Cu-Ga phase. If the Pd and Zn are spread over a large volume (low concentration) it may be difficult to detect these elements by use of EDS. These elements may also be difficult to detect if they are concentrated along grain boundaries. In this latter case they may be detected in a SEM, but not in TEM due to the larger analysed volumes in SEM.

4. Conclusions

The present work has shown that the investigated dental material consists of remaining undissolved particles from the Ag-based alloy powder in a matrix of reaction products with the liquid Ga alloy. Between the particles and the matrix reaction zones were found. The particles consist of orthorhombic Ag_3Sn. In the matrix the following phases were found: cubic Ag_9In_4, tetragonal β-Sn and hexagonal Ag_2Ga. The reaction zones were found to consist of two types: the cubic γ-Cu_9Ga_4 and Ga-rich Cu-Ga regions which are intergrowths of the tetragonal $CuGa_2$ and one of the γ-Cu_9Ga_4 phases. The crystalline phases identified by use of TEM in the present work, their space group and cell dimensions are given in Table III. The space groups and cell dimensions can be found in Villars and Calvert [25].

As mentioned earlier, X-ray diffraction has previously been used to identify the phases in this dental Ga alloy. Some disagreements between the TEM and X-ray results have been found. In Table VI the phases identified by use of X-ray diffraction is summarized [11]. The major differences between the results from the X-ray diffraction study and the present TEM investigation are the following.

TABLE III Space group and cell dimensions of the identified phases in the dental Ga alloy found in the present work

Phase	Space group	Cell dimensions (nm)		
		a	*b*	*c*
Ag_3Sn	Pmmn	0.5968	0.47802	0.51843
Ag_2Ga	$P\bar{6}$	0.77677		0.28778
Cu_9Ga_4	$P\bar{4}3m$	0.8747		
Ga-Cu intergrowth				
Ag_9In_4	$P\bar{4}3m$	0.9922		
Sn	$I4_1/amd$	0.58318		0.31819

TABLE IV Space group and cell dimensions of the identified phases in the dental Ga alloy as found by Herø *et al.* [11]

Phase	Space group	Cell dimensions (nm)		
		a	*b*	*c*
ζ-Ag_3Sn	$P6_3/mmc$	0.2970		0.4774
ζ′-Ag_3Sn	Pmmn	0.4801	0.4780	0.3048
ζ-Ag_6Ga_3	P3	0.7736		0.2872
θ-Cu(Pd) Ga_2	P4/mmm	0.2818		0.5796
γ-Ag_9In_4	P43m	0.9830		
β-Sn	$I4_1/amd$	0.5799		0.3171

According to Herø *et al.* [11] the particles consist of both an orthorhombic (ζ′) and a hexagonal (ζ) phase of Ag_3Sn, whereas only the orthorhombic (ε) phase was found in the TEM study. There are also differences in composition and cell dimensions of the orthorhombic (ζ′) and (ε) phases. The ζ′-phase has cell dimensions: $a = 0.4801$ nm, $b = 0.4780$ nm and $c = 0.3048$ nm whereas the ε-phase has: $a = 0.5968$ nm, $b = 0.47802$ nm and $c = 0.51843$ nm. Two axes are approximately equal in the two structures, but the third axis is doubled in ε-phase compared to the ζ′-phase.

Another difference between the results of the two investigations concerns the presence of the Ga-rich Cu-Ga regions. According to Herø *et al.* [11] the reaction zones around the particles consist of a tetragonal θ-Cu(Pd)Ga_2 phase and a cubic Cu_9Ga_4 phase. The cubic phase was also found in the present TEM work, but instead of the tetragonal θ-Cu(Pd)Ga_2 phase the Ga-rich Cu-Ga regions consist of an intergrowth between the tetragonal $CuGa_2$ and one of the cubic γ-Cu_9Ga_4 phases. No indication of Pd was found in these regions.

According to Herø *et al.* [11] the β-Sn phase appears as white particles in matrix and contains a substantial amount of Ga, In and Ag. The maximum solubility of Ga and In in Sn according to the binary phase diagrams was in agreement with their experimental observations, whereas the measured content of Ag and Cu in β-Sn was higher than expected from the binary phase diagrams. According to Herø *et al.* [11] this discrepancy could "be due to either small precipitates not visible by SEM or interference from surrounding phases". In the present TEM work almost pure Sn was found to cover large areas, but some small particles in the β-Sn phase were also seen. According to the EDS analyses these particles are Ag-rich.

References

1. PUTTKAMMER, *Zahnärztliche Rundschau* **35** (1928) 1450.
2. D. L. SMITH and H. J. CAUL, *J. Amer. Dent. Assoc.* **53** (1956) 315.
3. National Institute of Health, in "Report from Technical Assessment Conference on Effects and Side Effects of Dental Restorative Materials" (Washington DC, August 1992).
4. R. C. WEAST(Ed.), "Handbook of physics and chemistry" (CRC Press Inc., Boca Raton, FL, 1986).
5. L. K. MASH, B. H. MILLER, H. NAKAJIMA, S. M. COLLARD and T. OKABE, *J. Dent. Res.* **71** (1992) 570.
6. T. OKABE, M. K. WOLDU and H. NAKAJIMA, *ibid.* **70** (1991) 343.
7. H. NAKAJIMA, B. H. MILLER, T. OKABE, *ibid.* **71** (1992) 570.
8. T. OKABE, M. WOLDU, H. NAKAJIMA, B. H. MILLER and L. K. MASH, *ibid.* **71** (1992) 688.
9. R. JØRGENSEN, H. HERØ, M. SYVERUD and L. SHUIPING, *ibid.* **73** (1993) 981.
10. International Organization for Standardization, ISO 1559 "Alloys for dental amalgam", 2nd Edn (Geneva, Switzerland 1986).
11. H. HERØ, C. J. SIMENSEN and R. B. JØRGENSEN, *Biomaterials* (1995) submitted.
12. C. W. FAIRHURST and J. B. COHEN, *Acta Crystallogr.* **B28** (1972) 371.
13. G. CLIFF and G. W. LORIMER, in Proceedings of the 5th. European Congress on Electron Microscopy (Institute of Physics, Bristol, 1972) p. 140.
14. A. OLSEN, in "The theory and practice of analytical electron microscopy in materials science" (Department of Physics, University of Oslo, Oslo, 1992).
15. R. STOKHUYZEN, J. K. BRANDON, P. C. CHIEH and W. B. PEARSON, *Acta Crystallogr.* **B30** (1974) 2910.
16. T. B. MASSALSKI, J. L. MURRAY, L. H. BENNET and H. BAKER, in "Binary alloy phase diagrams" (American Society for Metals, Ohio, 1986).
17. F. WEIBKE, *Z. anorg. chem.* **220** (1934) 293.
18. E. ZINTL and O. TREUSCH, *Z. Physik. Chem.* **B34** (1936) 225.
19. J. O. BETTERTON JR. and W. HUME-ROTHERY, *J. Inst. Metals* **80** (1951–1952) 459.
20. M. EL-BORAGY and K. SCHUBERT, *Zeit. für Metall.* **63** (1972) 52.
21. J. K. BRANDON, R. Y. BRIZARD, W. B. PEARSON and D. J. N. TOZER, *Acta Crystallogr.* **B33** (1977) 527.
22. V. T. DESHPANDE and D. B. SIRDESHMUKH, *ibid.* **14** (1961) 355.
23. K. KOMATSU and K. TERAMOTO, *J. Phys. Soc. Jpn.* **21** (1966) 1152.
24. R. P. STRATTON and W. J. KITCHINGMAN, *Acta Crystallogr.* **17** (1964) 1471.
25. P. VILLARS and L. D. CALVERT, in "Pearson's handbook of crystallographic data for intermetallic phases" (American Society for Metals, Ohio, 1985).

Received 21 August
and accepted 7 September 1995